Journal of Microbiological Methods 169 (2020) 105833

Contents lists available at ScienceDirect

Journal of Microbiological Methods

journal homepage: www.elsevier.com/locate/jmicmeth

An evaluation of the impact of clinical bacterial isolates on epithelial cell monolayer integrity by the electric Cell-Substrate Impedance Sensing (ECIS) method

Md A. Nahid[a,*], Carmen E. Campbell[b], Keith S.K. Fong[b], Jason C. Barnhill[c], Michael A. Washington[c]

[a] United States Army Institute of Surgical Research, San Antonio, TX, United States
[b] Department of Clinical Investigation, Tripler Army Medical Center, Honolulu, HI, United States
[c] Department of Chemistry and Life Science, United States Military Academy, West Point, NY, United States

ARTICLE INFO

Keywords:
Bacteria
Infection
Invasion
Resistance
Virulence

ABSTRACT

Virulence is the relative capacity of a pathogenic microorganism to cause damage in susceptible host cells such as those found in airway passages and the gut. In this study, the effect of clinical bacterial isolates on the monolayer integrity of cultured human alveolar basal epithelial cells (A549) was evaluated using the Electric Cell-Substrate Impedance Sensing (ECIS) system. ECIS is a morphological biosensor which records electrical properties of cell-covered microelectrodes in an AC circuit including impedance (ohm), resistance (ohm), and capacitance (μFarad). In the current study, fluctuations in the electrical properties of cell-covered microelectrodes reflect dynamic changes in cell morphology resulting from disrupted cell monolayers following exposure to bacteria. Using the ECIS system, real-time changes of cell morphology and disruption of monolayer integrity of cell-cultures *in vitro* were revealed for A549 cells infected with either *Pseudomonas aeruginosa,* ESBL *Escherichia coli*, *Staphylococcus aureus* (MRSA), or *Enterococcus* (VRE). We determined empirically that the optimal signal response was obtained for resistance (ohm) measurements at 4000 hertz. Following infection of A549 cells, the data revealed that *Pseudomonas aeruginosa* resulted in little change in microelectrode resistance (ohm @4 kHz) as compared to pathogen-free controls within the first 12 h. In contrast, *E. coli*, MRSA, and VRE caused significant changes in electrode resistance (ohm @4 kHz) values in the infected cells compared to controls over the first 5 h. Resistance (ohm @4 kHz) changes were also observed in cell monolayers infected with different bacterial concentrations for all isolates over 24 h. The highest concentration of bacteria caused the measured resistance (ohm @4 kHz) to drop faster than its' immediate lower concentration, suggesting a dose-dependent effect. Compared to live bacteria, cells exposed to heat-killed bacteria did not show significant changes in resistance (ohm @4 kHz) over 48 h post-exposure.

Functionally, cytokine responses were different between cells treated with live and heat-killed bacteria. Of note, live bacteria induced IFNγ, IL-13, and IL-1β production in A549 cells, whereas heat-killed bacteria induced IL-8 production suggesting a differential interaction with cells that could reveal the underlying causes of resistance (ohm @4 kHz) changes. Our findings indicate that ECIS provides a means to quantify, automate, and measure bacterial virulence, which may have broader implications governing the course of treatment compared to traditional methods alone.

1. Introduction

Bacterial infection is a significant cause of morbidity and mortality in the healthcare setting (Cornejo-Juarez et al., 2015; Travers and Barza, 2002). The recent emergence of drug resistant organisms in both community related and hospital-acquired infections has increased the significance of bacterial infection with respect to the full spectrum of healthcare (Barrasa-Villar et al., 2017). In addition, bacterial infections

Abbreviations: ECIS, Electric Cell-Substrate Impedance Sensing; ESBL, Extended-spectrum beta-lactamases; HK, Heat-killed; MRSA, Methicillin-resistant *Staphylococcus aureus*; PSAE, *Pseudomonas aeruginosa*; VRE, Vancomycin-resistant *Enterococcus faecalis*

* Corresponding author at: 3698 Chambers Pass BLDG 3611, JBSA Fort Sam Houston, TX 78234, United States.
E-mail address: md.a.nahid.mil@mail.mil (M.A. Nahid).

https://doi.org/10.1016/j.mimet.2020.105833
Received 20 May 2019; Received in revised form 30 December 2019; Accepted 1 January 2020
Available online 02 January 2020
0167-7012/

increase the overall cost of health care by complicating mechanical trauma and lengthening hospital stays (Cosgrove, 2006; Cosgrove and Carmeli, 2003; Roberts et al., 2010). Quantifying the disruption of cell monolayers by bacterial pathogens is a surrogate measure of virulence. This is due to the fact that virulent pathogens tend to degrade tissue barriers and disperse throughout the body. It has been shown that the ability of pathogens to invade host tissues is responsible for the spread and dissemination of these pathogens within the host (Sansonetti, 1991). At present, the clinical laboratory does not have the ability to monitor the disruptive phenotype of bacterial pathogens, to determine whether antimicrobial therapy is capable of blocking cell monolayer disruption, or to detect changes in the invasive phenotype of bacterial populations over time.

Furthermore, the world is currently on the verge of the post-antibiotic era, an era which some have termed "Antibiotic Armageddon" (Kunin, 1997). In order to dissipate the effects of widespread resistance, the rational and efficient use of the current antibiotic armamentarium is essential. The Clinical Microbiology Laboratory provides resistance data to physicians and generates the antibiograms which are utilized to determine treatment options and modify the formulary. The most common methods including, disk diffusion testing, minimum inhibitory concentration testing, the *E*-test (epsilometer method), VITEK 2 (bioMérieux Inc., Durham, NC) and MicroScan WalkAway (Dade MicroScan Inc., Sacramento, CA) automated systems are used for identifying microorganisms and their susceptibility to antibiotics (Jorgensen and Ferraro, 2009).

While these methods are sufficient for determining *in vitro* minimum inhibitory concentrations of the various antibiotics they do not evaluate the ability of clinical isolates to disrupt cell monolayers and therefore do not provide insights regarding their level of virulence. Determining the level of virulence may help guide clinical decision making. For example, knowing that the cause of a wound infection is a highly virulent pathogen capable of disrupting cell monolayers, the physician may elect a more rigorous course of treatment than if the pathogen was not capable of invading cell monolayers. Furthermore, the ability to determine whether an antibiotic is capable of blocking cell monolayer disruption even if it is not capable of blocking *in vitro* growth of a bacterial pathogen will allow physicians to develop novel antibiotic therapies and to better determine whether a given agent is clinically relevant (Rubens et al., 1992). This ability may allow a broader spectrum of antibiotics to remain in the formulary. Additionally, a real-time method for measuring cell monolayer integrity *in vitro* may prove beneficial for evaluation of older antibiotics and to determine the therapeutic potential of off-label uses and repurposing current members of the hospital formulary.

Although, various *in vivo* and *in vitro* assays are available to determine virulence capacity, the Electric Cell-Substrate Impedance Sensing (ECIS) system is an ideal tool for evaluating dynamic changes at the cellular level in the clinical microbiology laboratory. The ECIS biosensor platform is capable of measuring impedance changes of cell-covered microelectrodes over a broad range of AC frequencies and was developed by Gieaver and Keese in 1991 (Giaever and Keese, 1991). The method is based on the fact that cells grown on the surface of gold microelectrodes (250 μm diameter) act as insulators resulting in measurable changes in impedance across the microelectrodes as shown diagrammatically in Fig. 1A (Xiao and Luong, 2003; Heijink et al., 2010). Subtle changes in cell morphology observed microscopically have been shown to result in significant changes in the electrical properties of cell-covered microelectrodes measured with ECIS as shown in Fig. 1B (Ko et al., 1998). Previously, cytopathic effects of virulence factors of microorganisms including viruses have been shown to alter impedance (ohm), resistance (ohm), and capacitance (μF) of cell-covered microelectrodes measured in real-time (Washington and Campbell, 2016; Campbell et al., 2007). The ECIS measurement is passive and independent of media resistance. Furthermore, the contribution of cell membrane potential to the measurement is negligible. The optimal measurement conditions for impedance (ohm), capacitance (μF), and resistance (ohm) can be determined empirically when measured across a range of frequencies.

We postulate that measured changes of electrical properties of cell-covered microelectrodes exposed to clinical bacterial isolates will have distinct values which will vary between bacterial strains and concentrations for infected cell cultures compared to pathogen-free controls. We also propose that the results from the current study may lay the foundation to screen for anti-bacterial agents for a broad spectrum of bacterial strains. Thus, to determine if ECIS can reveal a difference in the virulence capacity of bacterial strains and isolates *in vitro*, the aim of this study is to correlate measured ECIS values of cell-covered microelectrodes exposed to live bacteria from clinical isolates compared to bacteria free and heat-killed controls. Furthermore, the microelectrodes were imaged microscopically to assess the monolayer integrity and compared to the ECIS data.

2. Materials and methods

2.1. Cell culture preparation

Human alveolar basal epithelial cells (A549 cells) were obtained from the American Type Culture Collection (Manassas, VA., USA). Cells were maintained by twice weekly passage in DMEM medium supplemented with 10% FBS (VWR, PA, USA) and 100 U/ml penicillin-streptomycin (Mediatech Inc., Manassas, VA) at 37 °C with 5% CO_2.

2.2. Electric Cell-Substrate Impedance Sensing (ECIS) measurements

The ECIS model was first presented and demonstrated in 1991(Giaever and Keese, 1991) and since has been tested and peer reviewed by many scientists around the globe (Ramasamy et al., 2014; Tran et al., 2013; Voiculescu et al., 2018). ECIS provides a novel means to explore cell morphology and barrier function. The multi-frequency scan mode allows one to use the measured impedance data to calculate parameters that can be directly related to cell morphological changes and correlated to specific culture conditions such as the introduction of a pathogen. Measuring complex impedance and using the data to model cell morphological changes is one of the unique features of ECIS and not a part of normal Transepithelial/transendothelial electrical resistance (TEER) measurements or simple impedance measurements conducted at a single frequency. In the current study, the established ECIS method and microelectrode arrays consisting of 8 wells with 10 gold microelectrodes (250 μm in diameter) per well were used for all assays (Applied Biophysics, NY, USA).

It is noted that the small size of the working microelectrode is critical for the sensitivity of the measurement where the current flow is constricted to the area of the microelectrode (250 μm diameter). Using the 8W10E arrays allows for more cells across the monolayer to be monitored simultaneously as compared to the 8W1E arrays which are more sensitive to the impedance fluctuations of just a few cells on a single microelectrode. The 8W10E arrays have 10× the surface area available to measure. All ECIS array wells were coated with 0.01% poly-L-lysine (Sigma-Aldrich, St. Louis, MO, USA), seeded with 2.5×10^5 A549 cells in complete media, and continuously monitored with ECIS.

Impedance fluctuations of cell-covered gold microelectrodes are easily recorded using ECIS. The fluctuations in the measured impedance values reflect cell morphological changes resulting from bacteria induced cell death. A well-established cell monolayer is vital before infecting the cells with bacteria; however, timing for monolayer formation can vary between 20 and 24 h. Thus, when measured parameter values of the cell-covered microelectrodes plateaued at approximately 20–24 h post incubation, the ECIS measurement was paused, cell culture medium was exchanged for fresh antibiotic-free medium, allowing cell debris to be washed away. Bacteria suspensions in antibiotic-free medium were immediately added to cell monolayers and ECIS

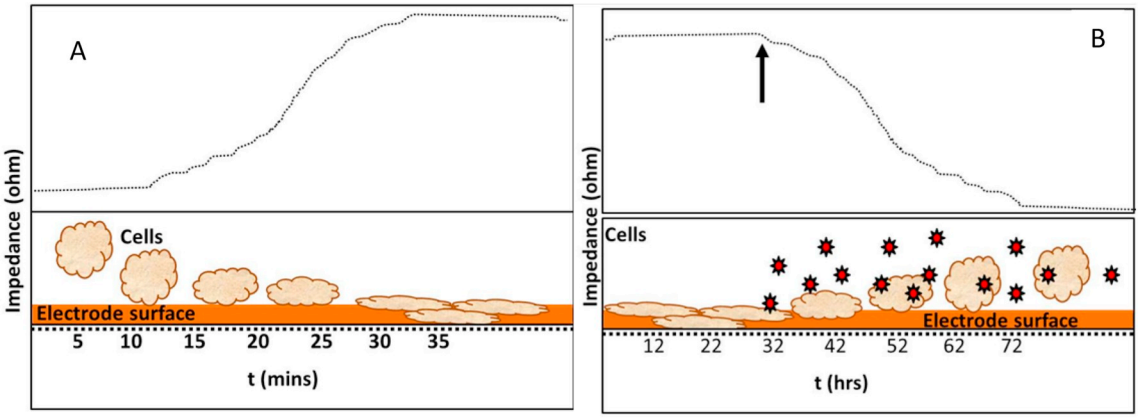

Fig. 1. Diagram illustrating the concept of measured impedance changes over time. In ECIS, impedance (ohm) increases are induced by cell adhesion and spreading across the microelectrode (A) and cytopathic effect resulting from the introduction of pathogens (arrow) shown in (B) induces a measurable decrease in impedance (ohm).

measurements were continued for up to 120 h.

Impedance (ohm), resistance (ohm), and capacitance (μF) values were recorded in series across the microelectrode arrays at 11 frequencies per well. All microelectrodes including pathogen-free and cell-free controls were monitored prior to and post pathogen introduction at frequencies ranging from 62.5 to 64 kHz (62.5, 125, 250, 500, 1000, 2000, 4000, 8000, 16000, 32000, 64000 Hz) using the multiple frequency time (MFT) mode. Recording the impedance, resistance, and capacitance values using the MFT mode also reveals the frequency where cells have the largest effect upon the measured parameters. This is determined by directly comparing the ratio of cell-covered microelectrode to the cell-free microelectrode measurements across all frequencies. Using the MFT course settings, it is also possible to determine the frequency where cells show the maximum response to a treatment condition. The maximum response for Impedance (Z), Resistance (R) and Capacitance (C) likely occurs at different frequencies. By default, the optimal frequencies are: Resistance (R (ohm)) @4 kHz; Impedance (Z (ohm)) @16 kHz; and Capacitance (C (μFarad)) @64 kHz. The optimal frequencies may also be obtained empirically by examining the data at each frequency. In the current study, we chose to present the resistance (ohm) values at 4 kHz since this was the optimal parameter and frequency determined empirically for evaluating cell response to bacterial challenge.

The data were analyzed using the Applied Biophysics *Z*-theta Analysis Software v1.2.92.0 (Taylor et al., 2013). Briefly, resistance (ohm) values obtained at 4 kHz were normalized using the analysis software by dividing each measured value (n) by the initial value (n_0), n/n_0 thus all values become one at time zero. Cell-covered, pathogen exposed microelectrodes were then compared to media only control microelectrodes and pathogen-free, cell-covered control microelectrodes. ECIS Z-theta analysis software was used to determine the resistance (ohm @4 kHz) values reflecting cell monolayer integrity and overall response to pathogenic bacteria.

In this study, A549 cell cultures were infected with four bacterial species, ESBL *Escherichia coli* (n = 16), Methicillin-resistant *Staphylococcus aureus* (MRSA, n = 14), Vancomycin-resistant *Enterococcus faecalis* (VRE, n = 17), and *Pseudomonas aeruginosa* (PSAE, n = 18). All isolates were derived from infected patients at the Tripler Army Medical Center. For baseline control condition, controls were included as growth media only (n = 20) or pathogen-free A549 cell monolayers (n = 20). Similarly, a series of diluted bacterial suspension starting OD_{600} at 1.0 (3.0×10^8 /ml) to 0.00001 was used to infect the cell monolayer. In addition to live bacterial infection, heat-killed bacteria were used to treat the cell monolayer following the same condition. Heat-killed (at 95 °C for 30 min) or live bacteria were used to treat A549 cell monolayers in parallel to live bacteria under the same experimental condition.

2.3. Multiplex analysis of bacteria induced cytokines

Twelve-well plates were seeded with A549 cells at 2.5×10^5 cells per well in complete DMEM with 10% bovine serum. Culture media was removed the following day, washed and replenished with or without bacterial suspensions. To each well 0.1 ml of an OD_{600} = 1.0 (3.0×10^8 /ml) bacterial suspension (live or heat-killed at 95 °C for 2 h) was added for a final volume of 2 ml culture medium and grown for 20 h. Culture medium was removed and centrifuged at 10,000 rpm for 10 min at 4 °C. Supernatants were carefully removed and filter-sterilized through a 0.2-μm syringe filtration disc. Aliquots of the supernatants (100 μL) were plated on blood agar plates to ensure negative growth. Filtered samples were stored at −80 °C until assay. Samples were thawed on ice just prior to conducting an immunology multiplex assay using the MILLIPLEX MAP human cytokine/chemokine magnetic bead panel (Millipore Sigma, Burlington, MA). For each sample, 1:2 and 1:3 dilutions (along with undiluted samples) were assayed in duplicate along with standards, quality controls and conditioned and unconditioned culture media according to the manufacturer's protocol. Assay plates were read and analyzed using the Luminex MAGPIX xMAP platform using xPONENT 4.2 and MILLIPLEX Analyst 5.1 software (Millipore Sigma).

2.4. Statistical analysis

Data are presented in the figures as mean ± SE. For multiple-group comparisons, a one-way analysis of variance (ANOVA/Tukey's test) was performed, followed by the two-sided, unpaired Student's *t*-test. The unpaired, two-tailed Student's t-test was used to compare two independent groups. For all statistical analyses, Prism for Windows, version 6.0 (GraphPad Software, San Diego, CA), was used, and a p value of 0.05 was considered statistically significant.

3. Results

3.1. Evaluation of A549 cell monolayer response to live bacteria

The ability of bacteria to disrupt and invade intercellular barriers can be determined by various approaches both *in vitro* and *in vivo*. However, most current approaches are time consuming, subjective, and do not necessarily provide real-time dynamic information reflecting cell behavior in presence of pathogens. Furthermore, alternative approaches to evaluate and quantify the virulence capacity of pathogens dynamically may in the future augment the ability to develop

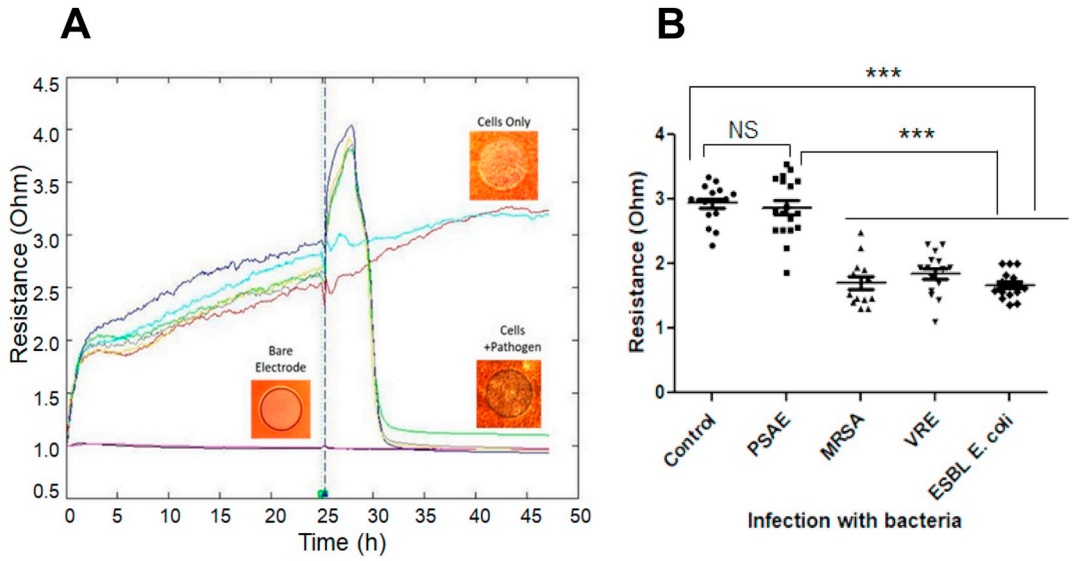

Fig. 2. Normalized electrode resistance of A549 cell monolayers with and without pathogen. (A) Confluent A549 cell monolayers washed with antibiotic-free medium were infected with MRSA in antibiotic-free medium and compared to pathogen-free controls. Normalized resistance (ohm @4 kHz) *versus* time curves of cell-free controls, pathogen-free controls, and pathogen exposed cell monolayers are shown. Microelectrode images were taken under a phase contrast inverted microscope at 200× magnification for each condition (inserts). (B) Normalized resistance (ohm @4 kHz) averaged over a 12 h window (p.i.) for the electrodes containing confluent A549 cell monolayers treated with bacteria (1.5×10^8 /ml) such as *P. aeruginosa* (PSAE, $n = 18$), Methicillin-resistant *S. aureus* (MRSA, $n = 14$), Vancomycin-resistant Enterococcus (VRE, $n = 17$), ESBL *E. coli* ($n = 16$) or left untreated (control, $n = 20$) in antibiotic-free medium are shown. Each isolate was run in triplicate. NS indicates non-significant. (***) indicates statistically significant difference (ANOVA/Tukey's test) between groups with $p < .001$. Dotted line (….) indicates the time at which the confluent cell monolayers were infected with bacteria.

therapeutic agents. The ECIS system was employed to determine whether the virulent nature of pathogens may be dynamically quantified by observing *in vitro* the ability of bacteria to disrupt established epithelial cell monolayers cultivated on the ECIS microelectrodes.

After recording the resistance (ohm @4 kHz) of the ECIS microelectrodes immersed only in cell culture medium, cells were seeded at 2.5×10^5 cells per well and incubated for approximately 24 h. Bacteria were introduced when the formation of a confluent monolayer was observed optically and reflected in the ECIS data as the resistance values plateaued over the time course of the experiment. In order to evaluate A549 cell monolayer response to MRSA exposure, MRSA was introduced at ~24-h after the wells were seeded with cells as shown in Fig. 2A. In most cases, resistance changes began within the first three hours post pathogen introduction and dropped to the level of the media-immersed cell-free microelectrodes (negative control) within 6 h. In contrast, under the same condition there was little change in measured resistance (ohm @4 kHz) of the uninfected A549 cell monolayer over the same time course. Using the same test conditions, isolates of four different bacterial species, *P. aeruginosa* (PSAE), MRSA, Vancomycin-resistant *Enterococcus* (VRE) and extended spectrum β-lactamase (ESBL) *E. coli* were evaluated. In Fig. 2B, a total of 18 PSAE isolates were used to infect the cell monolayers. However, about 66% (12/18) of the tested strains did not produce noticeable resistance (ohm @4 kHz) changes over 12 h (data not shown). This difference might be attributable to the species variation and their associated hemolytic capacity and other virulence factors. Thus, the normalized resistance (ohm @4 kHz) values for microelectrodes containing PSAE infected A549 cells showed insignificant differences compared to the microelectrodes containing uninfected cell monolayers (negative control, $n = 20$) over the initial 12 h window analyzed. In contrast, established monolayers exposed to the MRSA isolates revealed that 92% (13/14) of the tested strains produced a noticeable decrease in measured microelectrode resistance (ohm @4 kHz) over 12 h (raw data not shown). These values were significantly different ($p < .0001$) compared to either uninfected control or PSAE infected cells. Similar to MRSA, 95% of the tested VRE (16/17) infected cells exhibited a noticeable drop in measured resistance (ohm @4 kHz) (raw data not shown), resulting in a significant difference ($p < .0001$) compared to both control and PSAE treated cells. Similarly, 100% of the tested ESBL *E. coli* (16/16) strains showed a noticeable decrease in measured resistance (ohm @4 kHz) in the infected cells (raw data not shown), resulting in a significant difference ($p < .0001$) compared to either control or PSAE infected cells. Of note, Fig. 2B illustrates a significant decrease in resistance (ohm @4 kHz) values averaged over a 12-h window post infection for all strains except for *P. aeruginosa*. This is likely due to the large initial increase in resistance observed post-inoculation. This initial increase in the measured resistance has been observed in previous ECIS experiments and is not well understood (Cavallini and Tarantola, 2018). The large increase in resistance over the first 5–6 h post-PSAE introduction brings the average resistance for these samples to a higher average value across the 12-h window even though the over-all resistance dropped sharply to cell-free control values within approximately 10 h. Data from our experiments provides empirical evidence that the ECIS system may be used to evaluate and quantify clinical bacterial isolates. Additionally, it may also be possible to detect virulence potential as reflected in barrier function changes revealed by using the ECIS modeling parameters.

3.2. Dose dependent effect on epithelial cell barrier function exposed to a range of bacterial concentrations

In nature, hosts are always exposed to low levels of microorganisms, which are usually cleared by innate immunity; however, a number of infectious microorganisms manage to survive through their virulence mechanisms (Thakur et al., 2019). Thus, the ability of bacteria to evade host defense mechanism results in bacterial overgrowth to infectious doses and impairs the host immune system. It is always pertinent to detect bacteria before overgrowth occurs, eliminating the overuse of antibiotics. To establish the optimal test conditions for assessing bacterial virulence using the ECIS system, we selected the most pathogenic and clinically relevant strains. Based on our findings which revealed that significant resistance (ohm @4 kHz) changes may be induced by a single dose of bacteria, a range of doses was evaluated to determine a dose response curve while monitoring the cell monolayer integrity.

In Fig. 3, epithelial cell monolayers were treated with different

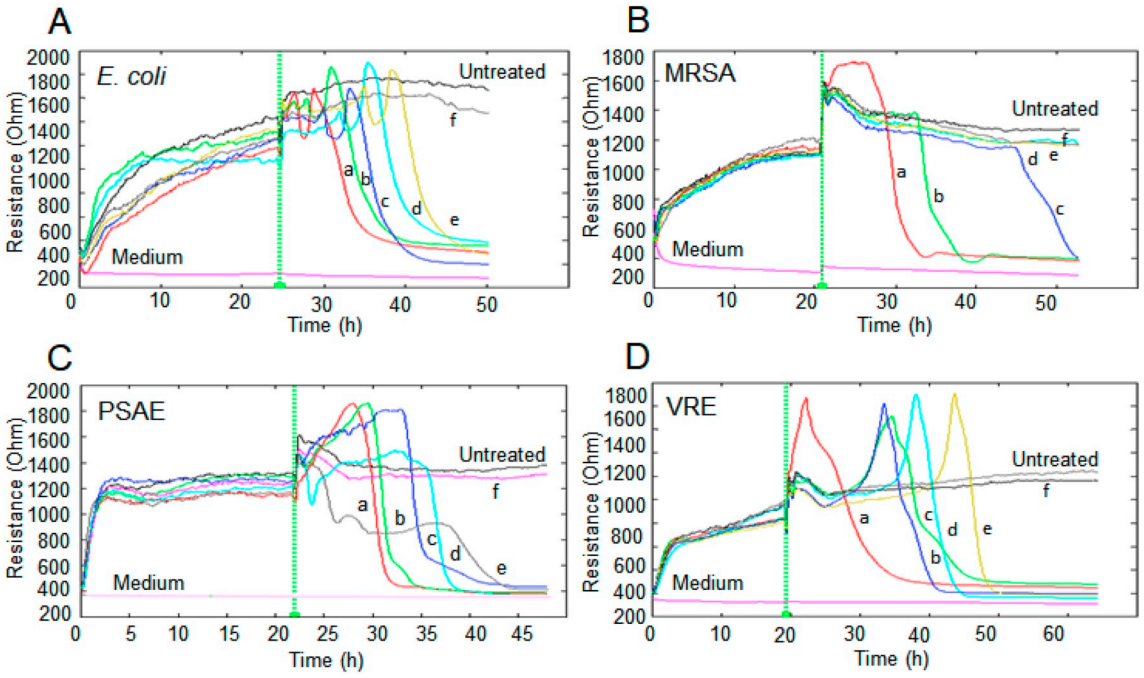

Fig. 3. Dose-dependent effect of bacterial disruption of A549 cell monolayer. Confluent monolayers in ECIS array wells were washed with antibiotic-free medium followed by infection with different doses of ESBL *E. coli* (A), MRSA (B), PSAE (C), and VRE (D) or left uninfected (negative control) for over 24 h. Each isolate was run in three independent experiments. Resistance (ohm @4 kHz) changes were shown for one of the representative experiments. At 600 nm, a = OD 1.0 (3.0×10^8/ml), b = OD 0.1, c = OD 0.01, d = OD 0.001, e = OD 0.0001, and f = OD 0.00001. Dotted line (….) indicates the time at which the confluent cell monolayers were infected with bacteria.

dilutions of the most disruptive ESBL *E. coli*, MRSA, PSAE, and VRE ranging from OD1.0 (3.0×10^8 bacteria /ml) to 0.00001 at OD_{600} over 24 h. Following infection, the disruption of the barrier function was reflected by a decrease in the microelectrode impedance and resistance using the ECIS system. Fig. 3A illustrates the response with the addition of a representative *E. coli* isolate to cell monolayers over a 24-h time point. Following infection, resistance (ohm @4 kHz) values began to drop within a couple of hours but declined dramatically at ~5 h after a brief increase in measured resistance (ohm @4 kHz). This pattern was the same for subsequent dilutions with noticeable changes observed at ~5 h for bacteria OD_{600} 1.0 (3.0×10^8 /ml), at 8 h for bacteria OD_{600} 0.1, at ~10 h for bacteria OD_{600} 0.01, at ~12 h for bacteria OD_{600} 0.001, and at ~14 h for bacteria OD_{600} 0.0001. Resistance (ohm @ 4 kHz) values approached baseline (similar to only media well read out) and stabilized over the course of 24 h post-infection. It is noted that there was little or no such change for bacteria OD_{600} 0.00001, which was similar to the uninfected control cells over the course of infection. In Fig. 3B, with the addition of a representative MRSA in cell monolayer at ~21 h, changes in microelectrode resistance (ohm) was noticed starting at ~6 h for bacteria OD_{600} 1.0 (3.0×10^8 /ml), followed by ~16 h and ~23 h for bacteria OD_{600} 0.1 and bacteria OD_{600} 0.01, respectively. However, there was little or no such change for bacteria OD_{600} 0.001 and at higher dilutions over 0.001, similar to uninfected cells over the course of ~30 h post-infection. In Fig. 3C, starting at 22 h post-infection of the cell monolayer with a representative PSAE, successive changes in microelectrode resistance (ohm @4 kHz) were noticed starting at ~6 h for bacteria OD_{600} 1.0 (3.0×10^8 /ml), at ~8 h for bacteria OD_{600} 0.1, at ~12 h for bacteria OD_{600} 0.01, at ~14 h for bacteria OD_{600} 0.001, at ~15 h for bacteria OD_{600} 0.0001, and at ~17 h for bacteria OD_{600} 0.00001. In Fig. 3D, with the addition of a representative VRE in cell monolayer, there was a successive change in measured resistance (ohm @4 kHz) values starting at ~3 h for bacteria OD_{600} 1.0 (3.0×10^8 /ml), at ~14 h for bacteria OD_{600} 0.1, at ~15 h for bacteria OD_{600} 0.01, at ~19 h for bacteria OD_{600} 0.001, and at ~25 h for bacteria OD_{600} 0.0001. However, no such changes were observed for bacteria OD_{600} 0.00001 over the course of 45 h post-infection, similar to the uninfected cell monolayer. Thus, these data indicate that virulence (or invasion) capacity was dependent on the number of infecting bacteria, which could be distinguished using the ECIS system.

3.3. Evaluation of heat-killed bacterial invasion capacity on A549 cell monolayer

The disruption of the monolayer can be due to the multifaceted functional effects of virulence factors on the cell. Most virulence factors are destroyed or altered by physical mechanisms such as heat, resulting in diminished virulence capacity to a certain extent. In order to support this idea, complete heat-killed (HK) bacteria with OD_{600} at 1.0 (3.0×10^8 /ml) were prepared (as described in Materials and Methods) and used to evaluate their cell disruption capacity in comparison with their respective live counterpart (3.0×10^8 /ml) by the ECIS system. In Fig. 4, HK PSAE, HK VRE, HK MRSA, and HK ESBL *E. coli* were used to treat confluent A549 cell monolayers in parallel to the respective live bacteria over 48 h. In Fig. 4A, live MRSA showed rapid changes in measured resistance (ohm) starting at 4 h and dropping down to the control (media well) level within 15 h of post-infection. In contrast, measured resistance (ohm @4 kHz) for the HK MRSA treated cells spiked upon addition, but leveled over the course of 60 h infection, which was similar to the uninfected cell monolayer. In Fig. 4B, live *E. coli* showed a measurable change in resistance (ohm @4 kHz) within the first 3 h and dropped almost to the level of negative controls (media well) within 24 h of post-infection. Interestingly, HK *E. coli* infected cells started showing measured resistance (ohm @4 kHz) changes at the same time of those infected with live bacteria, but dropped to about half of the live infected cells as the recorded microelectrode resistance (ohm @4 kHz) was 1200 Ω *vs.* 700 Ω, which remained the same level over 48 h of post-infection. In Fig. 4C, live VRE infected cells showed changes at 4 h and dropped to the level of negative controls (media well) within 20 h of post-infection. In contrast, HK VRE did not show

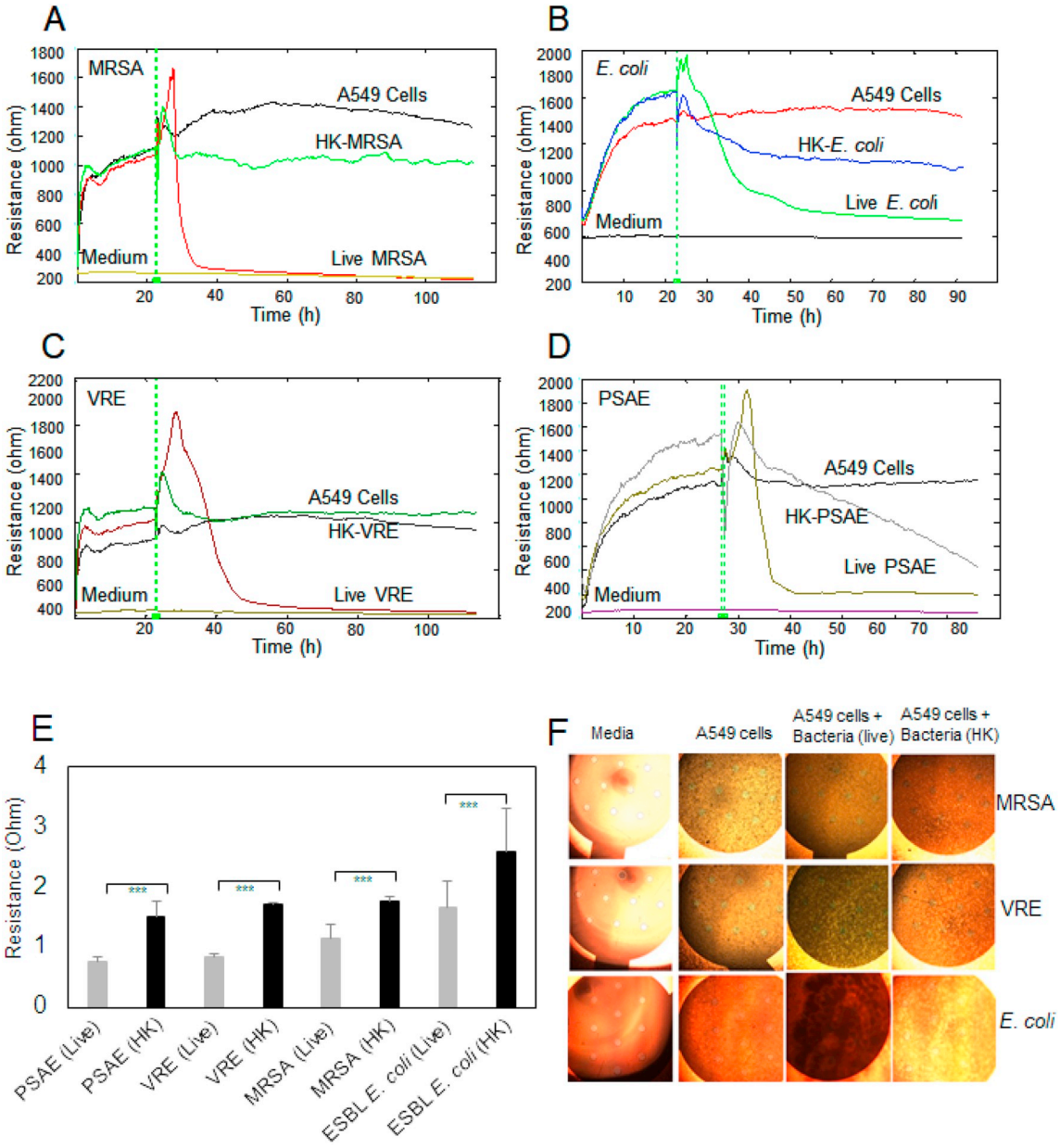

Fig. 4. Heat-killed bacterial invasion of cell monolayer. Resistance ((ohm) @4 kHz) values measured for up to 5 days are shown for confluent cell monolayers in ECIS array wells washed with antibiotic-free medium followed by treating with heat-killed (HK) MRSA or live MRSA (A), HK *E. coli* or live *E. coli* (B), HK VRE or live VRE (C), HK PSAE or live PSAE (D). Each isolate was run in triplicate wells. Calculated normalized peak resistance (ohm @4 kHz) for HK or live bacteria treated cells compared to cell-free media (E). Using a phase contrast inverted microscope, images were taken at 200× magnification for untreated or post-infected cell monolayer in the ECIS array wells (F). Results are expressed as ± SD from three independent experiments. $*p < .05$, $**p < .01$ compared between HK bacteria treatment *vs.* live bacterial infection. Dotted line (….) indicates the time at which the confluent cell monolayers were treated with live or HK bacteria.

any such change over the course of 48 h of post-infection, which was similar to the HK MRSA treated cell or uninfected cell control. In Fig. 4D, live PSAE infected cell showed changes starting at 3 h of post-infection and dropped to the control (medium well) level within 12 h. Although, changes in measured resistance (ohm @4 kHz) values started at 3 h for HK PSAE treated cells, it did not drop down to the level of cells infected with live bacteria until 60 h of post-infection. In Fig. 4E, the normalized resistance (ohm @4 kHz) values showed a higher value for HK PSAE, which was found to be significantly different compared to live PSAE ($p < .01$). Similarly, significant differences of normalized resistance (ohm @4 kHz) ($p < .01$) were also observed for HK VRE, MRSA, and *E. coli* compared to their respective live counterpart under the same conditions. In order to reveal the effect of live bacterial infection or HK bacteria treatment on the cell viability, images were taken under a phase contrast inverted microscope at 200× magnification (Fig. 4F). Of note, HK bacteria treated A549 cells remained viable (> 80%), almost similar to the uninfected cells. In contrast, as expected live bacteria infected cells were found to be dead, which was also checked by trypan blue exclusion assay (data not shown). Results from our experiments suggest that ECIS is a useful tool to distinguish the capacity for live *versus* heat-killed bacteria to disrupt a cell monolayer. Furthermore, our results confirmed that monolayer disruption is weakened or eliminated upon heat treatment.

3.4. Inflammatory response of A549 cell monolayers stimulated by live or dead bacteria

Bacteria or cellular components are potent stimulators of

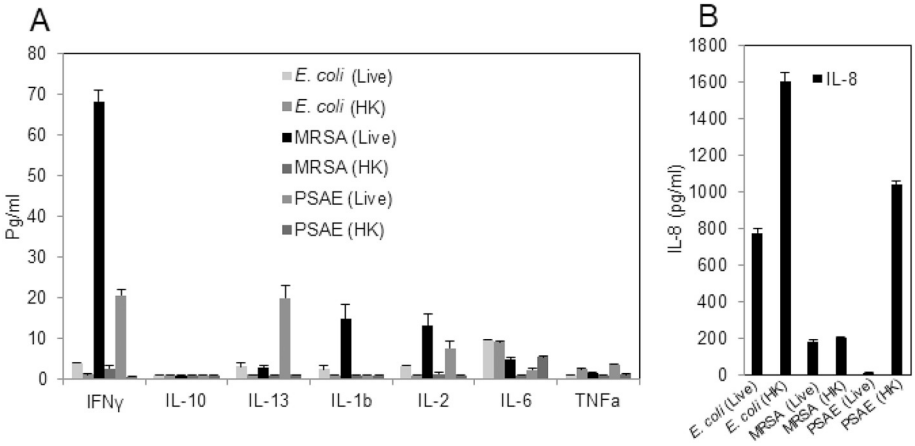

Fig. 5. HK or live bacterial stimulation and infection of A549 cells and induction of pro-inflammatory cytokines or chemokines. A549 cells were stimulated with same number (3.0×10^7 bacteria /well) of HK or live *E. coli*, MRSA, PSAE, and VRE for up to 24 h. At 24 h post-stimulation, supernatants were collected and picogram/ml concentrations of IFNγ, IL-10, IL-13, IL-1β, IL-2, IL-6, and TNF-α (A) or IL-8 (B) were measured by multiplex ELISA assay as described in Materials and Methods. Data points and error bars represent mean ± S.D. from 3 technical replicates from 1 of 2 independent experiments.

monocytes, macrophages, and epithelial cells (Nahid et al., 2009; Nahid et al., 2011a). Bacteria and their components have been shown to induce the expression of a diverse array of inflammatory mediators *in vitro* as well as under *in vivo* or *ex vivo* conditions (Nahid et al., 2011b; Ghosh et al., 2006). These infections lead to tissue injury and sustainable infection. Thus, the capacity for HK *vs.* live *E. coli*, *S. aureus*, and *P. aeruginosa* to induce A549 cell monolayers to express and secrete pro-inflammatory cytokines was evaluated (Fig. 5). With the exception of interleukin-8 (IL-8), there was no observed difference for other tested cytokine responses between the live and HK *E. coli* stimulated A549 cells (Fig. 5A–B). The amount of IL-8 was two-times greater in HK *E. coli* treated cells than that of infected with live *E. coli* (1638 pg/ml *vs.* 759 pg/ml) (Fig. 5B). Compared to HK MRSA, live MRSA treated cells resulted in a greater production of IFNγ (70 pg/ml), IL-1β (17 pg/ml) and IL-2 (15 pg/ml) (Fig. 5A). However, there was little, or no difference observed for other tested cytokines. Compared to HK PSAE, live PSAE treated cells showed more production of IFNγ (21 pg/ml), IL-13 (17 pg/ml), IL-2 (9 pg/ml), and TNF-α (3.7 pg/ml). HK PSAE was a potent inducer for IL-8 (1027 pg/ml *vs.* 10 pg/ml) in epithelial cell, which is similar to a previous report (Shanks et al., 2010). Thus, live and HK bacteria did not show similar cytokine responses because of differential interaction with epithelial cells that might lead to variable capacity to disrupt the cell monolayer integrity.

4. Discussion

Since the invention of ECIS (Giaever and Keese, 1991; Keese et al., 2004), it has been applied to biophysical and biomedical problems relating to barrier function, cell motility, cell-cell and cell-substrate adhesion and has been extensively reviewed (Heileman et al., 2013). Over the past two decades, ECIS has been applied to detect the attachment and spreading of cells to functionalized surfaces or cell-cell adhesion upon differentiation (Schafer et al., 2013; Rosman et al., 2014), directed migration, electroporation and wound healing (Keese et al., 2004; Yang et al., 2016; Schafer et al., 2011), as well as micromotion and barrier formation of metastatic cancer cells or cell cultures exposed to nanotoxic environments (Tramontini Gomes de Sousa et al., 2017; Schneider et al., 2011; Lovelady et al., 2007).

A biosensor for mammalian cell applications, called microelectromechanical systems (MEMS), detects microphysiological changes such as heat generated by a single mammalian cell or very small number of cells (Voiculescu et al., 2018). In contrast, ECIS is a passive measurement which records impedance, resistance, and capacitance over a range of frequencies in an alternating current (AC) circuit of cell-covered electrodes reflecting cell behavior and the different applications have been reviewed by Voiculescu et al. (Voiculescu et al., 2018). Another technology called xCELLigence, is similar to ECIS but does not take measurements in as many ways as the ECIS system does (Bischoff et al., 2016; Wei et al., 2012). Based on the biological applications of these technologies, ECIS is the most preferred method to investigate our experimental design. Although ECIS technology has been used to probe many fundamental questions of cell behavior in various conditions, it has not been investigated from bench side to clinical practice for evaluation of bacterial virulence or considered as a tool for optimization of antimicrobials to treat infection. In the present study, the ECIS system was primarily used to investigate the dynamic changes associated with the disruption of lung epithelial cell monolayer integrity upon exposure to clinically important isolates, which may provide insights for its potential benefit in the clinical setting.

Fibroblasts have been used for many types of assays using ECIS methodology (Cavallini and Tarantola, 2018). Cell monolayer formation plays a critical role for ECIS based assays and thereby cells were grown on the ECIS array well until stabilization of measured resistance (ohm @4 kHz) prior to introduction of bacterial isolates. In the current study, frequently encountered pathogenic bacteria in hospital environments were selected for the ECIS assays. The data revealed a significant difference in measured microelectrode resistance (ohm @ 4 kHz) values between uninfected cells and cells exposed to pathogens. Each bacterial strain showed unique changes in measured resistance (ohm @4 kHz) for cell-covered microelectrodes which provides a basis for understanding the degree of virulence. This response also reflected differences between pathogenic strains invading A549 cell monolayer. Initially in wells exposed to *P. aeruginosa*, the microelectrode resistance (ohm @4 kHz) increased significantly before subsequently decreasing. A number of *P. aeruginosa* isolates took > 12 h to disrupt the cell monolayer as reflected by the drop toward baseline in the measured microelectrode resistance (ohm @4 kHz) shown in Fig. 4D, suggesting strain differences, such as the differential nature of hemolysin, invasion capacity, and cytotoxicity (Fleiszig et al., 1995; Fleiszig et al., 1994). This could also differ in other cell lines as well as bacterial species and strains; however, more studies are needed to understand this behavior. In contrast to the PSAE response, *E. coli*, *S. aureus*, and *Enterococcus* spp. induced an immediate decrease in the measured microelectrode resistance (ohm) values while a brief or no initial increase was noted. The gradual decrease of measured resistance reflects morphological changes resulting from cell death as demonstrated by microscopic observation. In fact, observations of the ECIS microelectrodes were performed at pre- and post-infection during the experiments. Bright field images were taken one hour before and 24 h after infection of the culture monolayer. Consistently, microscopic observation of the *P. aeruginosa* infected A549 cell showed little or no death until resistance (ohm @4 kHz) values dropped down to the level of culture media without bacteria (data not shown).

Virulence of pathogenic organisms can be attributed to many categories such as the ability to enter a host, to evade host defenses, to grow in a host environment, to counteract host immune responses, to acquire

iron and nutrients from the environment and to sense environmental changes (Casadevall and Pirofski, 2009). There are many studies demonstrating that bacterial virulence depends on the infectious dose (Ong and Yim, 2017). Taking into account our above findings that changes in electrical properties of cell-covered microelectrodes were caused by a single dose of bacteria, a range of the bacterial concentrations were also used to investigate how these changes correlate to bacterial load. Our results confirmed that disruption of cell monolayers is dependent upon the bacterial load in the inoculum as well as the type of bacteria the cells are exposed to *in vitro*. Our observation supports the fact that measured changes of resistance (ohm) across the microelectrodes are due to the functional effect of live bacteria load on cell monolayer. Of note, the highest dilutions (0.00001 or higher) did not show any impedance changes over 48 h post-infection. It is noted that in Figs. 3 and 4D, cell-covered microelectrodes exposed to *P. aeruginosa* exhibited a significant initial increase in resistance (ohm) at 4 kHz over the first 10 h of the experiment at which point the measured resistance rapidly declined. Furthermore, the resistance for all samples was averaged over the first 12 h post inoculation as shown in (Fig. 2B). For the *P. aeruginosa* samples especially, this included the initial increase in resistance which was also noted for the other samples although the shape of the curves varied according to the taxa. The results from our experiments suggest that the initial resistance (ohm) magnitude and duration varies across taxa, is dose dependent, and necessitates further investigation. The microbial determinants that mediate damage in the context of microbial pathogenicity and virulence are the virulence factors which may have slight variations across isolates. The virulence capacity depends on one or a combination of several virulence factors including, capsular polysaccharide, capsule, DNAse, coagulase, fibrinolysin, proteolytic enzymes, hemolysin, bacteriocin production, hemagglutination, serum sensitivity, epithelial cell attachment, hydrophobicity, lipase, antiphagocytic factor, biofilm, extracellular enzymes production, presence of surface layer, lysine decarboxylase production and pili (Casadevall and Pirofski, 2009; Ong and Yim, 2017). Pathogenic bacteria possess one or more of those factors enabling them to cause disease in a susceptible host. Virulence factors are often targets of the immune response and the response to virulence factors can neutralize their action and provide host immunity. These virulence factors including the cytoplasmic membrane, proteins, ribosomes, and/or DNA are known to be denatured or altered by various physical mechanisms, including heat (Cangelosi and Meschke, 2014). Consistently, in this study, heat-killed bacteria caused little or no change in measured resistance (ohm) values of cell-covered microelectrodes even at 48 h post-exposure. However, the response was not as dramatic in the heat-killed *E. coli* and *P. aeruginosa* samples as the resistance (ohm) signal continued to drop slowly suggesting that further investigation is warranted. Since viable cells or intact virulence components may play an important role in cell monolayer disruption as reflected by measured resistance (ohm) changes of cell-covered microelectrodes, further investigation at the molecular level should be pursued in a future study.

Cytokines are known to contribute to changes in cell barrier function and impair host immunity. For example, IFNγ causes changes in epithelial barrier function (or cell integrity) that facilitates bacterial invasion and their subsequent adverse effect on host cells (Ahn et al., 2018). On the contrary, few cytokines including, IL-22 are known to protect cell integrity (Ahn et al., 2018). Previously, cytokine responses were observed for various types of heat-killed and live bacterial stimulation in monocytes or fibroblasts (Nahid et al., 2011b; Nahid et al., 2015). In our study, cytokine expression was found to be different between live and dead bacterial stimulation in the epithelial cells. Among the tested cytokines, IFNγ, IL-13, and IL-1β production was upregulated in cells exposed to live bacteria, while IL-8 production was upregulated in cells exposed to heat-killed bacteria. IL-8 is expressed by several cell types in response to inflammation (Nahid et al., 2015). It is noted that A549 cells have been shown to possess TLR5 receptor, which is specific for flagellin. *P. aeruginosa* flagellin has been shown to be important for binding to TLR5 and downstream NF-κB activation and proinflammatory cytokine or chemokine production, including IL-8 (Gewirtz et al., 2001; Takeuchi et al., 2003). Another study has shown that glycosylated flagellins are more effective than non-glycosylated flagellins for IL-8 production while exposed to A549 cells (Verma et al., 2005).

In our study, live *P. aeruginosa* (PSAE) infected A549 cells produced less IL-8 compared to heat-killed PSAE stimulated A549 cells, suggesting a significant impact of bacterial integrity to interact with TLR5. Compared to live mucoid bacteria, heat-killed PSAE might have more exposed flagellins, which are readily available to interact with TLR5. This could be the basis for the difference in IL-8 release between heat-killed and live bacteria observed in this study. However, the ability of flagellins to stimulate IL-8 production can vary depending on clinical isolates as well as the interacting cell types (Shanks et al., 2010), suggesting further investigation. IL-8 attracts neutrophils, basophils, and T-cells, but not monocytes. IL-8 is also involved in neutrophil activation. However, a direct role of IL-8 in regulating epithelial cell integrity is unknown. Compared to *in vitro*, *in vivo* or *ex vivo* cell destruction capacity by heat-killed and live bacteria treatment can be different. Thus, the production and nature of the cytokines and other unknown factors could play a role in disruption of cell monolayer barrier function. Additionally, many factors could lead to the difference of the cell monolayer disruption capacity between live and dead bacteria as reflected by the ECIS measurements. Discrimination between invasive and non-invasive or pathogenic *versus* non-pathogenic bacteria following antibiotic treatment is a logical application of this technology and has great potential for translation into clinical practice. For example, a given antibiotic may not block the growth of an organism on an agar plate, but if it stops the invasion of the organism into the host tissues this would prevent escape from immune surveillance and may result in elimination *via* the adaptive immune response.

In summary, our study demonstrates that the ECIS system can be used for monitoring and quantifying the virulence capacity of bacteria reflected in microelectrode resistance (ohm @4 kHz) changes in bacteria exposed cell monolayers *in vitro*. Each bacterial strain revealed a unique resistance (ohm @4 kHz) change pattern which provides a basis for future research in tracking pathogen associated diseases. It is interesting to speculate that the ECIS system can be used as a future rapid diagnostic tool for assessing the degree of virulence while preventing mortality or morbidity from infectious diseases.

Disclaimer

The views expressed herein are those of the author and do not reflect the position of the United States Military Academy, the Department of the Army, or the Department of Defense.

Acknowledgements

This work was supported by the Army Advanced Medical Technology Initiative (AAMTI) through Telemedicine and Advanced Technology Research Center (TATRC) at the US Army Medical Research and Materiel Command. Opinions, interpretations, conclusions and recommendations are those of the author and are not necessarily endorsed by the US Army. This research protocol was approved by the Tripler Army Medical Center Scientific Review Committee.

References

Ahn, D., Wickersham, M., Riquelme, S., Prince, A., 2018. The effects of IFN-lambda on epithelial barrier function contribute to *K. pneumoniae* ST258 Pneumonia. Am. J. Respir. Cell Mol. Biol. 60 (2), 158–166.

Barrasa-Villar, J.I., Aibar-Remon, C., Prieto-Andres, P., Mareca-Donate, R., Moliner-Lahoz, J., 2017. Impact on morbidity, mortality, and length of stay of hospital-acquired infections by resistant microorganisms. Clin. Infect. Dis. 65, 644–652.

Bischoff, I., Hornburger, M.C., Mayer, B.A., Beyerle, A., Wegener, J., Furst, R., 2016.

Pitfalls in assessing microvascular endothelial barrier function: impedance-based devices versus the classic macromolecular tracer assay. Sci. Rep. 6, 23671.
Campbell, C.E., Laane, M.M., Haugarvoll, E., Giaever, I., 2007. Monitoring viral-induced cell death using electric cell-substrate impedance sensing. Biosens. Bioelectron. 23, 536–542.
Cangelosi, G.A., Meschke, J.S., 2014. Dead or alive: molecular assessment of microbial viability. Appl. Environ. Microbiol. 80, 5884–5891.
Casadevall, A., Pirofski, L.A., 2009. Virulence factors and their mechanisms of action: the view from a damage-response framework. J. Water Health 7 (Suppl. 1), S2–S18.
Cavallini, F., Tarantola, M., 2018. ECIS based wounding and reorganization of cardiomyocytes and fibroblasts in co-cultures. Prog. Biophys. Mol. Biol. 144, 116–127.
Cornejo-Juarez, P., Vilar-Compte, D., Perez-Jimenez, C., Namendys-Silva, S.A., Sandoval-Hernandez, S., Volkow-Fernandez, P., 2015. The impact of hospital-acquired infections with multidrug-resistant bacteria in an oncology intensive care unit. Int. J. Infect. Dis. 31, 31–34.
Cosgrove, S.E., 2006. The relationship between antimicrobial resistance and patient outcomes: mortality, length of hospital stay, and health care costs. Clin. Infect. Dis. 42 (Suppl. 2), S82–S89.
Cosgrove, S.E., Carmeli, Y., 2003. The impact of antimicrobial resistance on health and economic outcomes. Clin. Infect. Dis. 36, 1433–1437.
Fleiszig, S.M., Zaidi, T.S., Fletcher, E.L., Preston, M.J., Pier, G.B., 1994. Pseudomonas aeruginosa invades corneal epithelial cells during experimental infection. Infect. Immun. 62, 3485–3493.
Fleiszig, S.M., Zaidi, T.S., Pier, G.B., 1995. Pseudomonas aeruginosa invasion of and multiplication within corneal epithelial cells in vitro. Infect. Immun. 63, 4072–4077.
Gewirtz, A.T., Simon Jr., P.O., Schmitt, C.K., Taylor, L.J., Hagedorn, C.H., O'Brien, A.D., Neish, A.S., Madara, J.L., 2001. Salmonella typhimurium translocates flagellin across intestinal epithelia, inducing a proinflammatory response. J. Clin. Invest. 107, 99–109.
Ghosh, T.K., Mickelson, D.J., Fink, J., Solberg, J.C., Inglefield, J.R., Hook, D., Gupta, S.K., Gibson, S., Alkan, S.S., 2006. Toll-like receptor (TLR) 2-9 agonists-induced cytokines and chemokines: I. comparison with T cell receptor-induced responses. Cell. Immunol. 243, 48–57.
Giaever, I., Keese, C.R., 1991. Micromotion of mammalian cells measured electrically. Proc. Natl. Acad. Sci. U. S. A. 88, 7896–7900.
Heijink, I.H., Brandenburg, S.M., Noordhoek, J.A., Postma, D.S., Slebos, D.J., van Oosterhout, A.J., 2010. Characterisation of cell adhesion in airway epithelial cell types using electric cell-substrate impedance sensing. Eur. Respir. J. 35, 894–903.
Heileman, K., Daoud, J., Tabrizian, M., 2013. Dielectric spectroscopy as a viable biosensing tool for cell and tissue characterization and analysis. Biosens. Bioelectron. 49, 348–359.
Jorgensen, J.H., Ferraro, M.J., 2009. Antimicrobial susceptibility testing: a review of general principles and contemporary practices. Clin. Infect. Dis. 49, 1749–1755.
Keese, C.R., Wegener, J., Walker, S.R., Giaever, I., 2004. Electrical wound-healing assay for cells in vitro. Proc. Natl. Acad. Sci. U. S. A. 101, 1554–1559.
Ko, K.S.C., Lo, C.M., Ferrier, J., Hannam, P., Tamura, M., McBride, B.C., Ellen, R.P., 1998. Cell–substrate impedance analysis of epithelial cell shape and micromotion upon challenge with bacterial proteins that perturb extracellular matrix and cytoskeleton. J. Microbiol. Methods 34, 125–132.
Kunin, C.M., 1997. Antibiotic armageddon. Clin. Infect. Dis. 25, 240–241.
Lovelady, D.C., Richmond, T.C., Maggi, A.N., Lo, C.M., Rabson, D.A., 2007. Distinguishing cancerous from noncancerous cells through analysis of electrical noise. Phys. Rev. E Stat. Nonlinear Soft Matter Phys. 76, 41908.
Nahid, M.A., Pauley, K.M., Satoh, M., Chan, E.K., 2009. miR-146a is critical for endotoxin-induced tolerance: IMPLICATION IN INNATE IMMUNITY. J. Biol. Chem. 284, 34590–34599.
Nahid, M.A., Satoh, M., Chan, E.K., 2011a. Mechanistic role of microRNA-146a in endotoxin-induced differential cross-regulation of TLR signaling. J. Immunol. 186, 1723–1734.
Nahid, M.A., Rivera, M., Lucas, A., Chan, E.K., Kesavalu, L., 2011b. Polymicrobial infection with periodontal pathogens specifically enhances microRNA miR-146a in ApoE−/− mice during experimental periodontal disease. Infect. Immun. 79, 1597–1605.
Nahid, M.A., Satoh, M., Chan, E.K., 2015. Interleukin 1beta-responsive MicroRNA-146a is critical for the cytokine-induced tolerance and cross-tolerance to toll-like receptor ligands. J. Innate. Immun. 7, 428–440.
Ong, H.S., Yim, H.C.H., 2017. Microbial factors in inflammatory diseases and cancers. Adv. Exp. Med. Biol. 1024, 153–174.
Ramasamy, S., Bennet, D., Kim, S., 2014. Drug and bioactive molecule screening based on a bioelectrical impedance cell culture platform. Int. J. Nanomedicine 9, 5789–5809.
Roberts, R.R., Scott 2nd, R.D., Hota, B., Kampe, L.M., Abbasi, F., Schabowski, S., Ahmad, I., Ciavarella, G.G., Cordell, R., Solomon, S.L., Hagtvedt, R., Weinstein, R.A., 2010. Costs attributable to healthcare-acquired infection in hospitalized adults and a comparison of economic methods. Med. Care 48, 1026–1035.
Rosman, C., Pierrat, S., Tarantola, M., Schneider, D., Sunnick, E., Janshoff, A., Sonnichsen, C., 2014. Mammalian cell growth on gold nanoparticle-decorated substrates is influenced by the nanoparticle coating. Beilstein J. Nanotechnol. 5, 2479–2488.
Rubens, C.E., Smith, S., Hulse, M., Chi, E.Y., van Belle, G., 1992. Respiratory epithelial cell invasion by group B streptococci. Infect. Immun. 60, 5157–5163.
Sansonetti, P.J., 1991. Genetic and molecular basis of epithelial cell invasion by Shigella species. Rev. Infect. Dis. 13 (Suppl. 4), S285–S292.
Schafer, E., Westendorf, C., Bodenschatz, E., Beta, C., Geil, B., Janshoff, A., 2011. Shape oscillations of Dictyostelium discoideum cells on ultramicroelectrodes monitored by impedance analysis. Small 7, 723–726.
Schafer, E., Tarantola, M., Polo, E., Westendorf, C., Oikawa, N., Bodenschatz, E., Geil, B., Janshoff, A., 2013. Chemotaxis of Dictyostelium discoideum: collective oscillation of cellular contacts. PLoS One 8, e54172.
Schneider, D., Tarantola, M., Janshoff, A., 2011. Dynamics of TGF-beta induced epithelial-to-mesenchymal transition monitored by electric cell-substrate impedance sensing. Biochim. Biophys. Acta 1813, 2099–2107.
Shanks, K.K., Guang, W., Kim, K.C., Lillehoj, E.P., 2010. Interleukin-8 production by human airway epithelial cells in response to Pseudomonas aeruginosa clinical isolates expressing type a or type b flagellins. Clin. Vaccine Immunol. 17, 1196–1202.
Takeuchi, K., Taguchi, F., Inagaki, Y., Toyoda, K., Shiraishi, T., Ichinose, Y., 2003. Flagellin glycosylation island in Pseudomonas syringae pv. glycinea and its role in host specificity. J. Bacteriol. 185, 6658–6665.
Taylor, S.L., Wahl-Jensen, V., Copeland, A.M., Jahrling, P.B., Schmaljohn, C.S., 2013. Endothelial cell permeability during hantavirus infection involves factor XII-dependent increased activation of the kallikrein-kinin system. PLoS Pathog. 9, e1003470.
Thakur, A., Mikkelsen, H., Jungersen, G., 2019. Intracellular pathogens: host immunity and microbial persistence strategies. J Immunol Res 2019, 1356540. https://doi.org/10.1155/2019/1356540.
Tramontini Gomes de Sousa Cardozo, F., Baimukanova, G., Lanteri, M.C., Keating, S.M., Moraes Ferreira, F., Heitman, J., Pannuti, C.S., Pati, S., Romano, C.M., Cerdeira Sabino, E., 2017. Serum from dengue virus-infected patients with and without plasma leakage differentially affects endothelial cells barrier function in vitro. PLoS One 12, e0178820.
Tran, T.B., Nguyen, P.D., Um, S.H., Son, S.J., Min, J., 2013. Real-time monitoring in vitro cellular cytotoxicity of silica nanotubes using electric cell-substrate impedance sensing (ECIS). J. Biomed. Nanotechnol. 9, 286–290.
Travers, K., Barza, M., 2002. Morbidity of infections caused by antimicrobial-resistant bacteria. Clin. Infect. Dis. 34 (Suppl. 3), S131–S134.
Verma, A., Arora, S.K., Kuravi, S.K., Ramphal, R., 2005. Roles of specific amino acids in the N terminus of Pseudomonas aeruginosa flagellin and of flagellin glycosylation in the innate immune response. Infect. Immun. 73, 8237–8246.
Voiculescu, I., Toda, M., Inomata, N., Ono, T., Li, F., 2018. Nano and microsensors for mammalian cell studies. Micromachines 9, 439.
Washington, M.A., Campbell, C.E., 2016. Phenotypic analysis of bacterial virulence using electric cell-substrate impedance sensing. MLO Med. Lab. Obs. 48 (30), 32.
Wei, P.L., Kuo, L.J., Wang, W., Lin, F.Y., Liu, H.H., How, T., Ho, Y.S., Huang, M.T., Wu, C.H., Chang, Y.J., 2012. Silencing of glucose-regulated protein 78 (GRP78) enhances cell migration through the upregulation of vimentin in hepatocellular carcinoma cells. Ann. Surg. Oncol. 19 (Suppl. 3), S572–S579.
Xiao, C., Luong, J.H., 2003. On-line monitoring of cell growth and cytotoxicity using electric cell-substrate impedance sensing (ECIS). Biotechnol. Prog. 19, 1000–1005.
Yang, J.M., Chen, S.W., Yang, J.H., Hsu, C.C., Wang, J.S., 2016. A quantitative cell modeling and wound-healing analysis based on the Electric Cell-substrate Impedance Sensing (ECIS) method. Comput. Biol. Med. 69, 134–143.